International Journal of Pure and Applied Physics.
ISSN 0973-1776 Volume 12, Number 1 (2016), pp. 53-60

http://www.ripublication.com

Synthesis and characterization of surfactant assisted CeO_2/ZrO_2 nanocomposite

S. Usharani* and V. Rajendran

Department of Physics, Presidency College, Chennai-05, Tamilnadu, India.
Corresponding author E-mail: sushamoorthy15@gmail.com

Abstract

This paper reports the synthesis of CeO_2/ZrO_2 nanocomposite by wet chemical method using cationic surfactant (CTAB). The properties of the obtained nanocomposites were analysed by X-ray diffraction (XRD), Fourier transform infrared (FTIR), scanning electron microscoy (SEM), transmission electron microscopy (TEM), UV-Diffuse Reflectance Spectroscopy (UV-DRS) and photoluminescence (PL) spectroscopy. XRD results confirm the formation of the crystalline nature and the mixed phase of CeO_2/ZrO_2 nanocomposites. FTIR and EDX results confirm the formation of Ce-O and Zr-O bond. The TEM studies revealed the spherical morphology of the CTAB assisted CeO_2/ZrO_2 nanocomposites in the size range of 26.8 nm. The UV-DRS studies revealed the bandgap value of CeO_2/ZrO_2 nanocomposites. The photoluminescence properties of CeO_2/ZrO_2 nanocomposites were observed in the strong UV region and several visible region peaks are likely to have originated from the oxygen vacancies.

Keywords: CeO_2/ZrO_2; CTAB; Wet chemical; Optical.

1. INTRODUCTION

ZrO_2 is an n-type semiconductor with wide band gap of Eg = 5.0eV is more valuable for important industrial applications such as photocatalytic, antibacterial, gas sensing and spintronic devices [1]. Recent research lies in doping and mixing metal oxide with ZrO_2, which enhance the applications in various fields. Various metal oxides mixed with ZrO_2, such as Bi_2O_3/ZrO_2, PbO_2/ZrO_2 and ZrO_2/V_2O_5 are used in different types of applications because of their enhanced optical and chemical properties [2-4]. In addition, cerium oxide (CeO_2) is a good rare earth photo catalyst with the band gap of 3.2eV and CeO_2 based materials have received much attention due to their

excellent physical and chemical properties, low cost and environment friendly feature. CeO_2 doped and mixed with various metal oxide show its potential applications such as photocatalytic activity, lithium ion batteries etc [5,6]. Likewise, ZrO_2 mixed with CeO_2, enhanced their properties and show their excellent photo catalytic activity, bio sensor etc [7-10]. Recent research interests lie in the morphological controlled synthesis of heterogeneous photocatalyst due to their enhanced properties and potential applications. This paper manifests the synthesis of CeO_2/ZrO_2 nanocomposite with well dispersed spherical morphology using cationic surfactant (CTAB) by wet chemical method. This wet chemical method is very simple, inexpensive, non toxic and yield high purity products. The properties of the prepared nanocomposites are characterized by different techniques such as XRD, FTIR, SEM, TEM, UV-DRS, PL, EDX, and SAED.

2. EXPERIMENTAL

2.1 Preparation of CeO_2/ZrO_2 nanocomposite

CeO_2/ZrO_2 nanocomposites were prepared by mixing of 0.1 M of cerrous chloride and zirconium oxy chloride octahydrate in water and stirred it for 30 min at room temperature to ensure the formation of the homogeneous mixed salt solution. Then cationic surfactant (CTAB) were added together and stirred for 1 h at room temperature. After the completion of 1 h the aqueous ammonium hydroxide solution was added dropwise to attain the pH-6.5 and stirred continuously for 2 hrs. The resultant product was dried for 12 hrs at 120^oC. After that, it was washed with water several times and then calcined at 600^oC for 8 hrs.

2.2 Characterisation

The XRD pattern of the nanopowder was recorded by using a powder X-ray diffractometer (Schimadzu model: XRD 6000 using CuKα (λ=1.5417 Å) radiation. The Fourier transform infrared (FTIR) spectra of the samples were taken using an FTIR model Bruker IFS 66 V spectrometer. High- resolution images and selected area electron diffraction patterns were observed by a JEOL JEM-2200FS transmission electron microscope (TEM) operating at 200 kV. The morphological studies of the samples were carried out by the SEM (Philips model CM 20) with EDX analysis. The optical absorption spectrum was obtained on a CARY 5E UV–VIS–NIR spectrophotometer. The photoluminescence emission spectra were carried out on a Fluoromax-4 spectrofluorometer with a Xe lamp as the excitation light source.

3. RESULTS AND DISCUSSION

The X-ray diffraction pattern of CTAB assisted CeO_2/ZrO_2 nanocomposite are shown in Fig. 1. The four peaks in the pattern with 2θ values of 29.8, 34.4, 49.6 and 59.1 correspond to the (101), (002), (022) and (203) planes which indicates the formation of tetragonal and monoclinic structure of ZrO_2 that are matched well with the reported values in JCPDS card 17-0923 and JCPDS card 37-1484. Similarly, the five peaks with 2θ values 28.6, 33.2, 47.6, 56.4 and 69.6 that are correspond to the (111), (200),

(220), (311) and (400) planes that indicates the formation of pure phase CeO_2 in a cubic fluorite structure [7,8]. Moreover, the XRD patterns exhibit the sharp peaks which reveal the well crystalline nature of the synthesized CeO_2/ZrO_2 nanocomposites. No peaks were observed due to the impurities which confirm the formation of pure CeO_2/ZrO_2 nanocomposite. The average crystallite size of the sample was calculated by using the Debye-Scherrer's equation (Equation 1) from full width at half maximum (FWHM) values of the CeO_2 and ZrO_2 planes.

$$D = \frac{0.89\,\lambda}{\beta \cos\theta} \tag{1}$$

Where λ represents the wavelength of the X-ray, θ indicates Bragg's angle, and β is the FWHM of the characteristic peaks. The average crystallite size of the sample was found to be 26.8 nm.

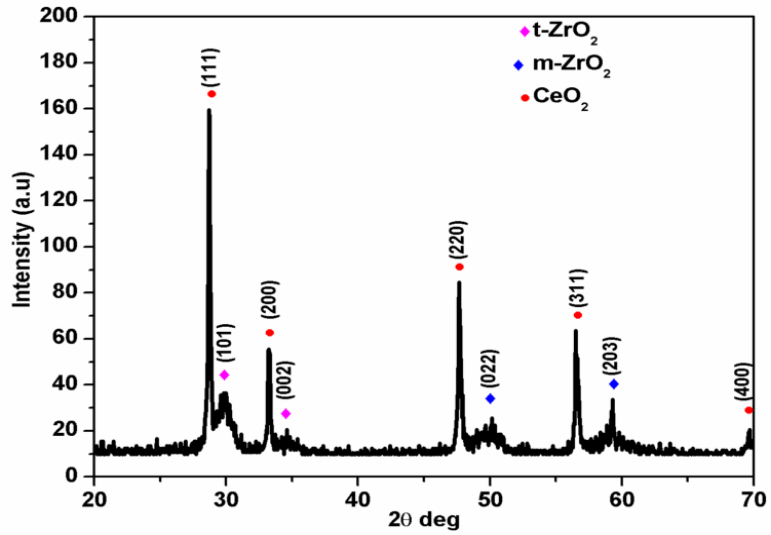

Fig. 1: XRD pattern of CTAB assisted CeO_2/ZrO_2 nanocomposite.

The FTIR spectrum of CeO_2/ZrO_2 sample prepared at three different pH values are shown in Fig. 2. From the spectra, the vibrational peaks observed at 3418 and 1639 cm^{-1} are due to the vibrations of –OH and H_2O functional groups. The absorption band observed in the region 549 cm^{-1} is associated with the stretching vibrations of Zr-O-Zr and Ce-O stretching vibration which are in close agreement with the reported values [11,12]. The band observed at 715 cm^{-1} is due to the Ce-Zr bridge formation, which is in close agreement with the reported literatures [13]. The peak observed at 2924 cm^{-1} can be attributed to the residual organic components.

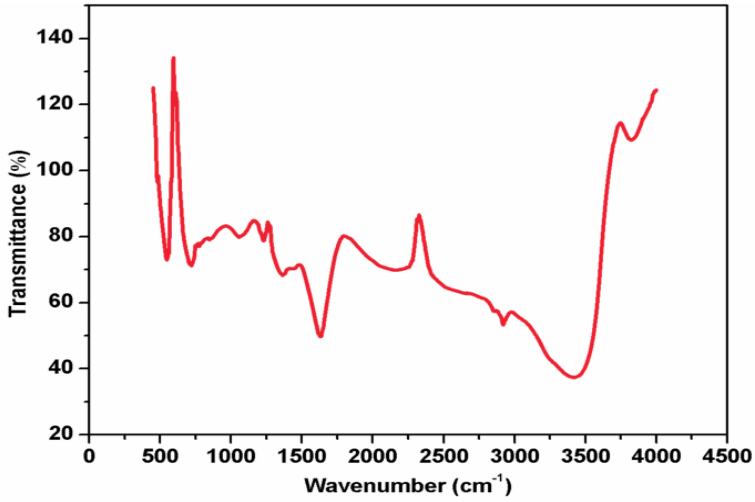

Fig. 2: FTIR spectrum of CTAB assisted CeO_2/ZrO_2 nanocomposite.

Fig. 3(a) shows the SEM micrograph of the CTAB assisted CeO_2/ZrO_2 nanocomposite. The SEM image shows the dispersed spherical morphologies were observed for the sample. The EDX spectra of CeO_2/ZrO_2 nanocomposite are presented in Fig. 3(b). The peaks corresponding to Zr, Ce and O are clearly observed in the EDX spectrum at their normal energy and the results are clearly indicating the formation of CeO_2/ZrO_2 nanocomposite.

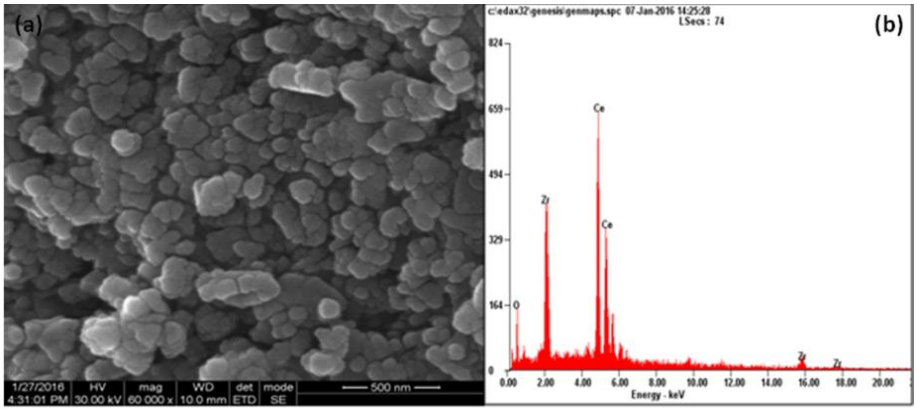

Fig. 3(a) SEM image and **Fig. 3(b)** EDX pattern of CTAB assisted CeO_2/ZrO_2 nanocomposite.

Fig. 4 shows the TEM image of CTAB assisted CeO_2/ZrO_2 nanocomposite. The well dispersed spherical morphologies were observed the TEM images. TEM result reveals the surfactant play key role to controlling the nucleation and crystal orientation. In the crystallization process, the surfactant molecules adsorbed on the crystal nuclei, as a result the dispersed spherical nanostructure were produced. The surfactant influences

the formation process and prevents the particle agglomeration. The SAED results clearly demonstrate the poly crystalline nature of the prepared sample as shown in the inset of Fig.4. The schematic formation of the CeO_2/ZrO_2 nanocomposites is shown in Fig. 5.

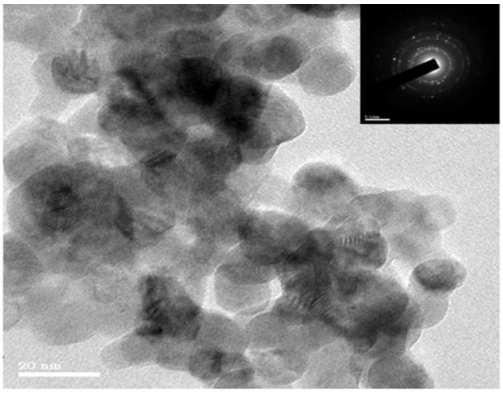

Fig. 4 TEM image of CTAB assisted CeO_2/ZrO_2 nanocomposite (SAED pattern inserted).

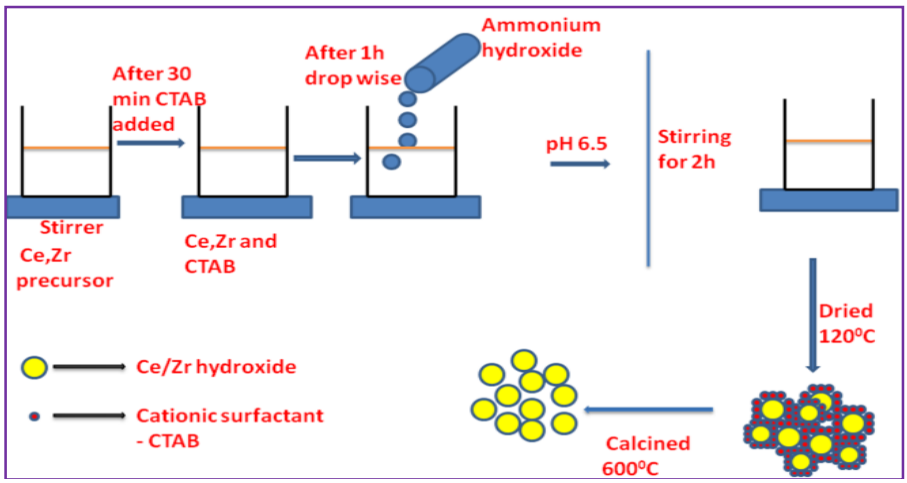

Fig. 5 Schematic formation of CTAB assisted CeO_2/ZrO_2 nanocomposite

The DRS-UV absorption spectrum of the CTAB assisted CeO_2/ZrO_2 nanocomposites are shown in Fig. 6 with absorption region at 409 nm. Further, the optical band gap energy of all prepared samples was calculated using the following relation.

$$E_g = \frac{hc}{\lambda}(eV) \quad (2)$$

Where, E_g represents the band gap energy (eV), h is the Planck constant, c is the velocity of light in meters and λ represents lower cutoff wavelength in nanometer. The corresponding band gap values are 3.03 eV. The shifted band gap value revealed

the formation of the mixed metal oxide CeO_2/ZrO_2 nanocomposites and it suggests a potential material for photocatalysis and opto-electronic devices [6].

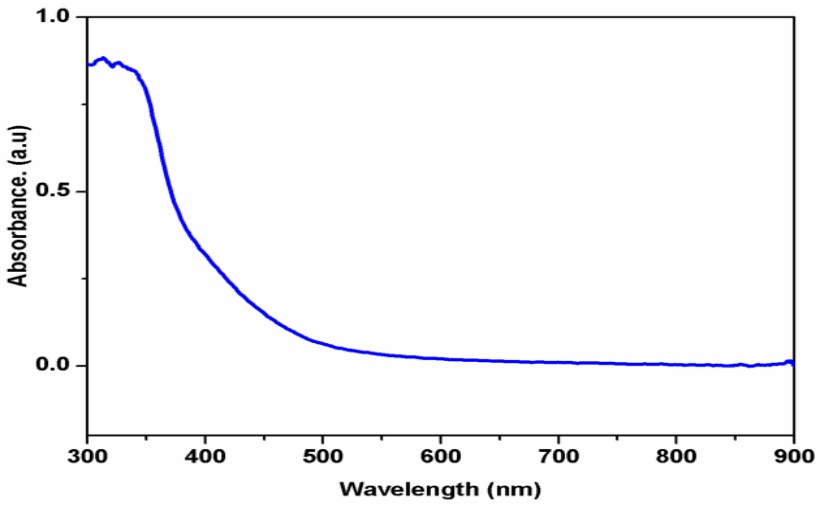

Fig. 6 UV-DRS spectrum of CTAB assisted CeO_2/ZrO_2 nanocomposite.

Fig. 7 shows the room temperature PL emission spectrum of the CTAB assisted CeO_2/ZrO_2 nanocomposites. The strong and weak UV emission peak at 323 and 396 nm is ascribed to the nearest band edge emission of the excitons. In addition, the strong blue green emission peak at 468 nm, weak blue green emission peaks appearing in 451, 484 and 494 nm, are likely to have transition in defect states [14]. Furthermore, it can be seen that the CTAB assisted CeO_2/ZrO_2 nanocomposites exhibit the higher luminescent peaks in both UV and visible region and it might be used for optoelectronic devices and photocatalytic applications.

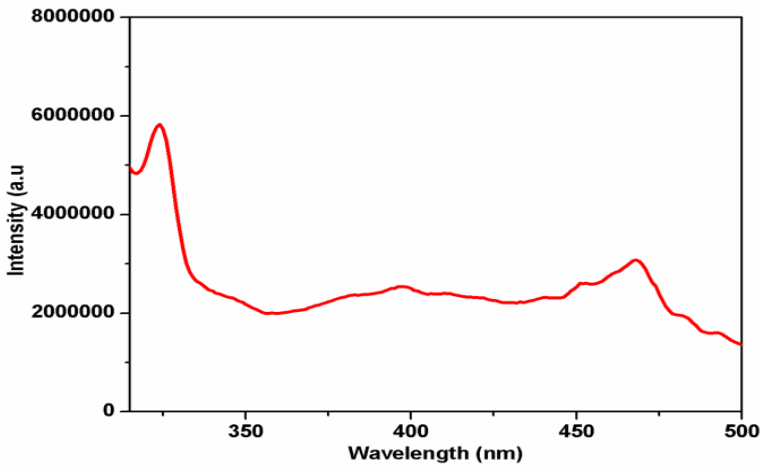

Fig. 7 Room temperature PL emission spectrum of CTAB assisted CeO_2/ZrO_2 nanocomposite.

4. CONCLUSION

In summary, nanocomposites of CeO_2/ZrO_2 with spherical morphology were prepared by using the wet chemical method together with CTAB as a surfactant. XRD and FTIR results confirm the formation of the well crystalline nature of ZrO_2 and CeO_2. The UV-DRS studies revealed the band gap of the CTAB assisted CeO_2/ZrO_2 nanocomposites and this result implying the improvement of surface oxygen vacancies may open up a new avenue for environmental remediation for the treatment of waste water and gas sensing. The PL results exhibit the CeO_2/ZrO_2 nanocomposites might be used for optoelectronic devices.

REFERENCES

[1] Kumar, S., and Ojha, A. K., 2015, "Oxygen vacancy induced photoluminescence properties and enhanced photocatalytic activity of ferromagnetic ZrO_2 nanostructures on methylene blue dye under ultra-violet radiation," J. Alloys Compd., 644, pp. 654-662.

[2] Vignesh, K., Priyanka, R., Rajarajan, M., and Suganthi, A., 2013, "Photoreduction of Cr(VI) in water using Bi_2O_3–ZrO_2 nanocomposite under visible light irradiation," Mater. Sci. Eng., B., 178, pp. 149-157.

[3] Yao, Y., Zhao, C., Zhao, M., and Wang, X., 2013, "Electrocatalytic degradation of methylene blue on PbO_2-ZrO_2 nanocomposite electrodes prepared by pulse electrodeposition," J. Hazard. Mater., 263, pp. 726-734.

[4] Padmamalini, N., and Ambujam, K., 2014, "Optical and dielectric properties of ZrO_2–V_2O_5 nanocomposites by co-precipitation calcinations method," Superlattices Microstruct., 76, pp. 376-384.

[5] Wang, Q., Huang, Y., Miao, J., Zhao, Y., and Wang, Y., 2013, "Synthesis and electrochemical characterizations of Ce doped SnS_2 anode materials for rechargeable lithium ion batteries," Electrochimica Acta., 93, pp. 120-130.

[6] Saravanan, R., Joicy, S., Gupta, V. K., Narayanan, V., and Stephen, A., 2013, "Visible light induced degradation of methylene blue using CeO_2/V_2O_5 and CeO_2/CuO catalysts," Mater. Sci. Eng., C. 33, pp. 4725-4731.

[7] Wang, X., Zhai, B., Yang, M., Han, W., and Shao, X., 2013, ZrO_2/CeO_2 nanocomposite: Two step synthesis, microstructure, and visible-light photocatalytic activity, Mater. Lett., 112, pp. 90-93.

[8] Pouretedal, H. R., Tofangsazi, Z., and Keshavarz, M. H., 2012, "Photocatalytic activity of mixture of ZrO_2/SnO_2, ZrO_2/CeO_2 and SnO_2/CeO_2 Nanoparticles," J. Alloys Compd., 513, pp. 359-364.

[9] Wang, Q., Gao, F., Zhang, X., Zhang, B., Li, S., Hu, Z., and Gao, F., 2012, "Electrochemical characterization and DNA sensing application of a sphere-like CeO_2-ZrO_2 and chitosan nanocomposite formed on a gold electrode by one-step electrodeposition," Electrochim. Acta., 62, pp. 250-255.

[10] Wang, J., Xu, W., Chen, L., Jia, Y., Wang, L., Huang, X-J., and Liu, J., 2013, "Excellent fluoride removal performance by CeO_2-ZrO_2 nanocages in water environment," Chem. Eng. J. 231, pp. 198-205.

[11] Sliem, M. A., Schmidt, D. A., Bétard, A., Kalidindi, S. B., Gross, S., Havenith, M., Devi, A., and Fischer, R. A., 2012, "Surfactant-Induced Nonhydrolytic Synthesis of Phase-Pure ZrO_2 Nanoparticles from Metal−Organic and Oxocluster Precursors," Chem. Mater., 24, pp. 4274-4282.

[12] Kalamuei, M. P., Alizadeh, S., Kamazani, M. M., and Niasari, M. S., 2015, "Synthesis and characterization of CeO_2 nanoparticles via hydrothermal Route," J. Ind. Eng. Chem., 21, pp. 1301-1305.

[13] Abo-Almaged, H. H., Khattab, R. M., and Sadek, H. E. H., 2016, "Preparation and Characterization of ZrO_2/CeO_2 Ceramic Composite Synthesized by Microwave Combustion Method," Oriental J. Chem., 32, pp. 243-251.

[14] Gnanamoorthi, K., Balakrishnan, M., Mariappan, R., and RanjithKumar, E., 2015, "Effect of Ce doping on microstructural, morphological and optical properties of ZrO_2 nanoparticles," Mater. Sci. Semicond. Process., 30, pp. 518-526.